JASEM ISSN 1119-8362

Full-text Available Online at
https://www.ajol.info/index.php/jasem
http://ww.bioline.org.br/ja

J. Appl. Sci. Environ. Manage.
Vol. 22 (6) 861 –866 June 2018

Compressibility of Air in Casting Mould Evaluated by Finite Element Method and the Stream Function Model

***INEGBEDION, F; AKPOBI, JA**

Department of Production Engineering, Faculty of Engineering, University of Benin, Benin City, Nigeria.
**Corresponding Author Email: francis.inegbedion@uniben.edu, +234-803-412-4035*

ABSTRACT: Casting is a manufacturing process for making complex shapes of metal materials. Casting has two stages – filling process requiring a gating system and solidification process requiring a riser. The air in the mould cavity during casting is displaced through the riser by the molten metal in a very rapid manner necessitating the need to determine its compressibility as it exit through the riser. The finite element method and the stream function model were used to analyze the flow of air through the top risers of casting mould. Results show that the velocity profile at any cross section is parabolic in shape with the maximum velocity at the centre. Comparing the finite element solutions with the exact solutions showed that the solutions converged towards the exact solutions. Further comparing of finite element solutions and experimental results with the local speed of sound (Mach number) showed that the Mach number was greater than one, which established that the air in the mould cavity during casting is compressible as it is displaced by the molten metal. Before now all researches did was to develop empirical equations and optimized molten metal flow in casting mould. This work has gone further to establish the compressibility of airflow in casting mould.

DOI: https://dx.doi.org/10.4314/jasem.v22i6.4

Dates: Received: 02 April 2018; Revised: 26 May: 2018; Accepted: 01 June 2018

Keywords: stream function, top riser, air, finite element

Casting a manufacturing process for making complex shapes of metal materials, have two main stages – filling process and solidification process (Feng, 2008). The filling process uses the gating system which composed of pouring cup, runner, sprue, sprue-well and ingate, is designed to guide liquid metal into the mould cavity. The solidification process uses the riser system to compensate for shrinkage caused by casting solidification (Feng, 2008). Apart from serving as a reservoir to compensate for shrinkage during solidification, the riser also serve as a channel through which the air displaced as a result of filling the mould cavity with the molten metal goes out of the mould cavity (Inegbedion and Akpobi, 2017a).

For the manufacturing engineer there are many situations where compressible flow understanding is essential for adequate design. These processes include situations not expected to have a compressible flow, such as casting and injection moulding (Meir, 2013). Casting is a process in which liquid metal is injected into a mould to obtain a near final shape. The air is displaced by the liquid metal in a very rapid manner, in a matter of milliseconds; therefore its compressibility has to be taken into account (Meir, 2013).

Porosity the most persistent and common complaint of casting users contributes directly to customer's concern about reliability and quality (Monroe, 2005). To control porosity an understanding of its source and causes is essential. One source of porosity in casting is a failure to eliminate all the air in the Mould Cavity during mould filling (Scott and Goodman, 1978). Aqida *et al*., (2004) examined the effects of porosity on mechanical properties of metal matrix composite and observed that porosity tends to decrease the mechanical properties of metal composite.

Peti and Grama, (2011) described porosity as trapped air in the casting which can come from several sources. Much work has been done to characterize the factors that causes porosity in casting, and to analyze the impact of porosity on the mechanical properties of metals (Aqida *et al.,* 2004). What has not yet been done is to analyze the behaviour of air (the main cause of porosity) in casting mould.

The aim of this work therefore was to determine the compressibility of air in casting mould as liquid metal is poured to fill the mould cavity using the finite element method and the stream function model.

MATERIALS AND METHODS

**Corresponding Author Email: francis.inegbedion@uniben.edu, +234-803-412-4035*

Finite Element Analysis (Reddy, 1993, 2006 and Singiresu, 2004). The model equation is the stream function model of axisymmetric flow of air in casting mould (Inegbedion and Akpobi, 2017b),

$$\frac{\partial^2\psi}{\partial z^2} = -\frac{\partial^2\psi}{\partial r^2} \quad (1)$$

The weighted residual of equation (1) is

$$N_i(r,z)\left(\frac{\partial^2\psi}{\partial z^2}+\frac{\partial^2\psi}{\partial r^2}\right)=0 \quad (2)$$

We integrated equation (2) over the element domain Ω_e

$$\int_{\Omega_e} N_i(r,z)\left(\frac{\partial^2\psi}{\partial z^2}+\frac{\partial^2\psi}{\partial r^2}\right)drdz = \int_{\Omega_e} N\left(\frac{\partial^2\psi}{\partial z^2}\right)drdz + \int_{\Omega_e} N\left(\frac{\partial^2\psi}{\partial r^2}\right)drdz$$
$$= \int_{\Omega_e} N\left(\frac{\partial}{\partial z}\right)\left(\frac{\partial\psi}{\partial z}\right)drdz + \int_{\Omega_e} N\left(\frac{\partial}{\partial r}\right)\left(\frac{\partial\psi}{\partial r}\right)drdz = 0$$

(3)

Let $\dfrac{\partial\psi}{\partial r}=\dfrac{\partial\psi}{\partial z}=H \quad (4)$

$$\therefore \int_{\Omega_e} N\left(\frac{\partial H}{\partial z}\right)drdz + \int_{\Omega_e} N\left(\frac{\partial H}{\partial r}\right)drdz = 0 \quad (5)$$

We integrated equation (5) by parts with respect to z and r using the basic relation

$$\int_{\Omega_e} udv = -\int_{\Omega_e} vdu + uv\big|_{\Omega_e} \quad (6)$$

and obtained equation (7)

$$\int_{\Omega_e}\left(\left(\frac{\partial[N]}{\partial z}\right)\left(\frac{\partial N}{\partial z}\right)+\left(\frac{\partial[N]}{\partial r}\right)\left(\frac{\partial N}{\partial r}\right)\right)drdz\{\psi\} = \int_{r_1}^{r_2} N(un_z - wn_r)d\Omega_e \quad (7)$$

The finite element model of equation (7) is given in matrix form as equation (8)

$$\left[K^e\right]\{\psi\} = \left|f^e\right| \quad (8)$$

$$\left[K^e\right] = \int_{\Omega_e}\left(\left(\frac{\partial[N]}{\partial z}\right)\left(\frac{\partial N}{\partial z}\right)+\left(\frac{\partial[N]}{\partial r}\right)\left(\frac{\partial N}{\partial r}\right)\right)drdz \quad (9)$$

$$\left|f^e\right| = \int_{r_1}^{r_2} N(un_z - wn_r)d\Omega$$

(10)

Let $(un_z - wn_r) = U_1$

Therefore, $\left|f^e\right| = \int_{r_1}^{r_2} N(U_1)d\Omega \quad (11)$

The stream function model over the domain of interest is discretized into finite elements having M nodes, using suitable interpolation model for $\psi^{(e)}$ in element e as (Reddy, 2006):

$$\psi \approx \psi(r,z) = \sum_{i=1}^{M} N_i(r,z)\psi_i = [N]\{\psi\} \quad (12)$$

The interpolation functions $N_i(r,z)$ are the same as those developed for linear rectangular elements, with $x = r$ and $y = z$ (Inegbedion and Akpobi, 2017b). This will enable us to evaluate the integrals of the K_{ij}^e and f_{ij}^e. Let's consider an approximation of the form:

$$N(r,z) = c_1 + c_2 r + c_3 z + c_4 rz \quad (13)$$

and using a rectangular element with sides a and b (Figure 1a).

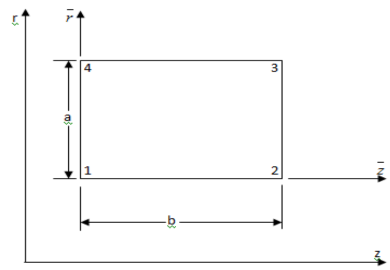

Fig 1a: Geometry of the element

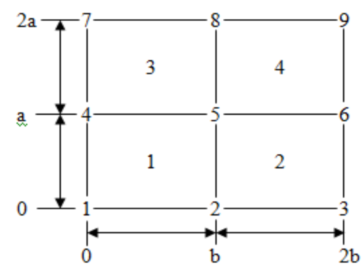

Fig 1b: Four Linear Rectangular Elements

We choose a local coordinate system (a,b) to derive the interpolation function. Thus equation (13) becomes

$$N(r,z) = c_1 + c_2 a + c_3 b + c_4 ab \quad (14)$$

and require $N_1 = N(0,0) = c_1$

$$N_2 = N(a,0) = c_1 + c_2 a$$
$$N_3 = N(a,b) = c_1 + c_2 a + c_3 b + c_4 ab$$
$$N_4 = N(0,b) = c_1 + c_3 b \quad (15)$$

Solving for $c_i\,(i = 1,\ldots,4)$, in equations (15) we obtained

$$c_1 = N_1 \quad c_2 = \frac{N_2 - N_1}{a} \quad c_3 = \frac{N_4 - N_1}{b} \quad c_4 = \frac{N_3 - N_4 + N_1 - N_2}{ab} \quad (16)$$

We substituted equation (16) into equation (14) and noting that $a = r$ and $b = z$, we obtained

$$N(r,z)=\left(1-\frac{r}{a}\right)\left(1-\frac{z}{b}\right)N_1+\frac{r}{a}\left(1-\frac{z}{b}\right)N_2+\frac{rz}{ab}N_3+\frac{z}{b}\left(1-\frac{r}{a}\right)N_4=\phi_1N_1+\phi_2N_2+\phi_3N_3+\phi_4N_4 \tag{17}$$

$$\phi_1=\left(1-\frac{r}{a}\right)\left(1-\frac{z}{b}\right)\qquad \phi_2=\frac{r}{a}\left(1-\frac{z}{b}\right)\qquad \phi_3=\frac{rz}{ab}\qquad \phi_4=\frac{z}{b}\left(1-\frac{r}{a}\right) \tag{18}$$

We differentiated equations (18) with respect to *r* and *z*

$$\frac{d\phi_1}{dr}=\left(-\frac{1}{a}\right)\left(1-\frac{z}{b}\right)=\left(\frac{-1}{a}+\frac{z}{ab}\right)\quad \frac{d\phi_1}{dz}=\left(-\frac{1}{b}\right)\left(1-\frac{r}{a}\right)=\left(\frac{-1}{b}+\frac{r}{ab}\right)\quad \frac{d\phi_2}{dr}=\frac{1}{a}\left(1-\frac{z}{b}\right)=\frac{1}{a}-\frac{z}{ab}$$

$$\frac{d\phi_2}{dz}=-\frac{r}{ab}\quad \frac{d\phi_3}{dr}=\frac{z}{ab}\quad \frac{d\phi_3}{dz}=\frac{r}{ab}\quad \frac{d\phi_4}{dr}=-\frac{z}{ab}\quad \frac{d\phi_4}{dz}=\frac{1}{b}\left(1-\frac{r}{a}\right)=\frac{1}{b}-\frac{r}{ab} \tag{19}$$

We rewrote [K^e] in equation (9) as the sum of four basic matrices and using the interpolation function of (19) evaluated the several K_{ij}^e of each matrix using Figures 1a & 1b

$$K_{ij}^e=\left(K^1+K^2+K^3+K^4\right) \tag{20}$$

$$K^1=\begin{bmatrix}K_{11}^1 & K_{12}^1 & K_{13}^1 & K_{14}^1\\ K_{21}^1 & K_{22}^1 & K_{23}^1 & K_{24}^1\\ K_{31}^1 & K_{32}^1 & K_{33}^1 & K_{34}^1\\ K_{41}^1 & K_{42}^1 & K_{43}^1 & K_{44}^1\end{bmatrix};\quad K^2=\begin{bmatrix}K_{11}^2 & K_{12}^2 & K_{13}^2 & K_{14}^2\\ K_{21}^2 & K_{22}^2 & K_{23}^2 & K_{24}^2\\ K_{31}^2 & K_{32}^2 & K_{33}^2 & K_{34}^2\\ K_{41}^2 & K_{42}^2 & K_{43}^2 & K_{44}^2\end{bmatrix};\quad \text{similarly for } K^3 \text{ and } K^4$$

$$K_{11}^1=\int_0^b\int_0^a\left[\left(\left(-\frac{1}{a}\right)\left(1-\frac{z}{b}\right)\right)^2+\left(\left(-\frac{1}{b}\right)\left(1-\frac{r}{a}\right)\right)^2\right]drdz=\frac{a}{3b}+\frac{b}{3a} \tag{21}$$

$$K_{12}^1=\int_0^b\int_0^a\left[\left(\frac{-1}{a}+\frac{z}{ab}\right)^2+\left(\frac{-1}{b}+\frac{r}{ab}\right)\left(-\frac{r}{ab}\right)\right]drdz=\frac{a}{6b}+\frac{b}{3a} \tag{22}$$

Similarly we evaluated all elements of K^1 matrix

$$K_{11}^2=\int_0^b\int_a^{2a}\left[\left(\left(-\frac{1}{a}\right)\left(1-\frac{z}{b}\right)\right)^2+\left(\left(-\frac{1}{b}\right)\left(1-\frac{r}{a}\right)\right)^2\right]drdz=\frac{a}{3b}+\frac{b}{3a} \tag{23}$$

$$K_{12}^2=\int_0^b\int_a^{2a}\left[\left(\frac{-1}{a}+\frac{z}{ab}\right)^2+\left(\frac{-1}{b}+\frac{r}{ab}\right)\left(-\frac{r}{ab}\right)\right]drdz=\frac{b}{3a}-\frac{5a}{6b} \tag{24}$$

Similarly we evaluated all elements of K^2 matrix

$$K_{11}^3=\int_b^{2b}\int_0^a\left[\left(\left(-\frac{1}{a}\right)\left(1-\frac{z}{b}\right)\right)^2+\left(\left(-\frac{1}{b}\right)\left(1-\frac{r}{a}\right)\right)^2\right]drdz=\frac{a}{3b}+\frac{b}{3a} \tag{25}$$

$$K_{12}^3=\int_b^{2b}\int_0^a\left[\left(\frac{-1}{a}+\frac{z}{ab}\right)^2+\left(\frac{-1}{b}+\frac{r}{ab}\right)\left(-\frac{r}{ab}\right)\right]drdz=\frac{a}{6b}+\frac{b}{3a} \tag{26}$$

Similarly we evaluated all elements of K^3 matrix

$$K_{11}^4=\int_b^{2b}\int_a^{2a}\left[\left(\left(-\frac{1}{a}\right)\left(1-\frac{z}{b}\right)\right)^2+\left(\left(-\frac{1}{b}\right)\left(1-\frac{r}{a}\right)\right)^2\right]drdz=\frac{a}{3b}+\frac{b}{3a} \tag{27}$$

$$K_{12}^{4} = \int_{b}^{2b}\int_{a}^{2a}\left[\left(\frac{-1}{a}+\frac{z}{ab}\right)^{2}+\left(\frac{-1}{b}+\frac{r}{ab}\right)\left(-\frac{r}{ab}\right)\right]drdz = \frac{-5a}{6b}+\frac{b}{3a} \tag{28}$$

Similarly we evaluated all elements of K^4 matrix

Equation (20) became

$$[K^{e}] = \left(\begin{bmatrix} \frac{a}{3b}+\frac{b}{3a} & \frac{a}{6b}+\frac{b}{3a} & \frac{-a}{6b}-\frac{b}{6a} & \frac{a}{3b}+\frac{b}{6a} \\ \frac{a}{6b}+\frac{b}{3a} & \frac{a}{3b}+\frac{b}{3a} & \frac{b}{6a}-\frac{a}{3b} & \frac{b}{6a}-\frac{a}{6b} \\ \frac{-a}{6b}-\frac{b}{6a} & \frac{b}{6a}-\frac{a}{3b} & \frac{a}{3b}+\frac{b}{3a} & \frac{a}{6b}-\frac{b}{3a} \\ \frac{a}{3b}+\frac{b}{6a} & \frac{b}{6a}-\frac{a}{6b} & \frac{a}{6b}-\frac{b}{3a} & \frac{a}{3b}+\frac{b}{3a} \end{bmatrix} + \begin{bmatrix} \frac{a}{3b}+\frac{b}{3a} & \frac{b}{3a}-\frac{5a}{6b} & \frac{5a}{6b}-\frac{b}{6a} & \frac{a}{3b}+\frac{b}{6a} \\ \frac{b}{3a}-\frac{5a}{6b} & \frac{7a}{3b}+\frac{b}{3a} & \frac{b}{6a}-\frac{7a}{3b} & \frac{b}{6a}-\frac{5a}{6b} \\ \frac{5a}{6b}-\frac{b}{6a} & \frac{b}{6a}-\frac{7a}{3b} & \frac{7a}{3b}+\frac{b}{3a} & \frac{5a}{6b}-\frac{b}{3a} \\ \frac{a}{3b}+\frac{b}{6a} & \frac{b}{6a}-\frac{5a}{6b} & \frac{5a}{6b}-\frac{b}{3a} & \frac{a}{3b}+\frac{b}{3a} \end{bmatrix} \right.$$
$$\left. + \begin{bmatrix} \frac{a}{3b}+\frac{b}{3a} & \frac{a}{6b}+\frac{b}{3a} & \frac{-a}{6b}+\frac{5b}{6a} & \frac{a}{3b}-\frac{5b}{6a} \\ \frac{a}{6b}+\frac{b}{3a} & \frac{a}{3b}+\frac{b}{3a} & \frac{-5b}{6a}-\frac{a}{3b} & \frac{5b}{6a}-\frac{a}{6b} \\ \frac{-a}{6b}+\frac{5b}{6a} & \frac{-5b}{6a}-\frac{a}{3b} & \frac{a}{3b}+\frac{7b}{3a} & \frac{a}{6b}-\frac{7b}{3a} \\ \frac{a}{3b}-\frac{5b}{6a} & \frac{5b}{6a}-\frac{a}{6b} & \frac{a}{6b}-\frac{7b}{3a} & \frac{a}{3b}+\frac{7b}{3a} \end{bmatrix} + \begin{bmatrix} \frac{a}{3b}+\frac{b}{3a} & \frac{-5a}{6b}+\frac{b}{3a} & \frac{5a}{6b}+\frac{5b}{6a} & \frac{a}{3b}-\frac{5b}{6a} \\ \frac{-5a}{6b}+\frac{b}{3a} & \frac{7a}{3b}+\frac{b}{3a} & \frac{-5b}{6a}-\frac{7a}{3b} & \frac{5b}{6a}+\frac{5a}{6b} \\ \frac{5a}{6b}+\frac{5b}{6a} & \frac{-5b}{6a}-\frac{7a}{3b} & \frac{7a}{3b}+\frac{7b}{3a} & \frac{-5a}{6b}-\frac{7b}{3a} \\ \frac{a}{3b}-\frac{5b}{6a} & \frac{5b}{6a}+\frac{5a}{6b} & \frac{-5a}{6b}-\frac{7b}{3a} & \frac{a}{3b}+\frac{7b}{3a} \end{bmatrix} \right) \tag{29}$$

Typical riser height is twice riser diameter (*H=2D*) for top risers opened to atmospheric pressure (Flinn 1963). The height (*z*) to diameter (*d*) ratio used in this work is *2:1*. Therefore, *b=z=2mm* and *a=r=0.5mm* and equation (29) became

$$[K^{e}] = \left(\begin{bmatrix} 1.4167 & 1.375 & -0.70833 & 0.75 \\ 1.375 & 1.4167 & 0.5833 & 0.625 \\ -0.70833 & 0.5833 & 1.4167 & -1.2917 \\ 0.75 & 0.625 & -1.2917 & 1.4167 \end{bmatrix} + \begin{bmatrix} 1.4167 & 1.125 & -0.4583 & 0.75 \\ 1.125 & 1.9167 & 0.0833 & 0.4583 \\ -0.4583 & 0.0833 & 1.9167 & -1.125 \\ 0.75 & 0.4583 & -1.125 & 1.4167 \end{bmatrix} + \right.$$
$$\left. \begin{bmatrix} 1.4167 & 1.375 & 3.2917 & -3.25 \\ 1.375 & 1.4167 & -3.4167 & 3.2917 \\ 3.2917 & -3.4167 & 9.4167 & -9.2917 \\ -3.25 & 3.2917 & -9.2917 & 9.4167 \end{bmatrix} + \begin{bmatrix} 1.4167 & 1.125 & 3.5417 & -3.25 \\ 1.125 & 1.9167 & -3.9167 & 3.5417 \\ 3.5417 & -3.9167 & 1.9167 & -9.5417 \\ -3.25 & 3.5417 & -9.5417 & 1.4167 \end{bmatrix} \right) \tag{30}$$

Next we evaluated the $\left|f^{e}\right|$ matrix using equation (11)

The velocity entering the boundary *ab* is U_1 = *1588.6288mm/s* (Inegbedion and Akpobi, 2017a) and hence the vector $\left|f^{e}\right|$ will be nonzero only for elements 1 and 3 (Figure 1b). These nonzero vectors can be computed as follows (Singiresu, 2004): $\left|f^{e}\right| = \int_{r_1}^{r_2} N(U_1)d\Omega = U_1\int_{r_1}^{r_2} N_i d\Omega = \frac{U_1\Omega_{ij}}{2}[N_i]$ (31)

Where Ω_{ji} denote the lengths of the edge *z*

$$\left|f^{1}\right| = \left(\frac{U_1\Omega_{ji}}{2}\right)\begin{Bmatrix} N_1^1 \\ N_2^1 \\ N_3^1 \\ N_4^1 \end{Bmatrix} = \left(\frac{U_1\Omega_{ji}}{2}\right)\begin{Bmatrix} 1 \\ 0 \\ 0 \\ 1 \end{Bmatrix} \quad \left|f^{2}\right| = \left|f^{4}\right| = 0 \quad \left|f^{3}\right| = \left(\frac{U_1\Omega_{ji}}{2}\right)\begin{Bmatrix} N_1^3 \\ N_2^3 \\ N_3^3 \\ N_4^3 \end{Bmatrix} = \left(\frac{U_1\Omega_{ji}}{2}\right)\begin{Bmatrix} 1 \\ 0 \\ 0 \\ 1 \end{Bmatrix} \tag{32}$$

We assembled the system matrix using Figure 1b and equation (8)

$$\begin{bmatrix} K_{11}^1 & K_{12}^1 & 0 & K_{14}^1 & K_{13}^1 & 0 & 0 & 0 & 0 \\ K_{21}^1 & K_{22}^1+K_{11}^2 & K_{12}^2 & K_{24}^1 & K_{23}^1+K_{14}^2 & K_{23}^2 & 0 & 0 & 0 \\ 0 & K_{21}^2 & K_{22}^2 & 0 & K_{24}^2 & K_{23}^2 & 0 & 0 & 0 \\ K_{41}^1 & K_{42}^2 & 0 & K_{44}^1+K_{11}^3 & K_{43}^1+K_{12}^3 & 0 & K_{14}^3 & K_{13}^3 & 0 \\ K_{31}^1 & K_{32}^1+K_{41}^2 & K_{42}^2 & K_{34}^1+K_{21}^3 & K_{33}^1+K_{44}^2+K_{22}^3+K_{11}^4 & K_{43}^2+K_{12}^4 & K_{24}^3 & K_{23}^3+K_{14}^4 & K_{13}^4 \\ 0 & K_{31}^2 & K_{32}^2 & 0 & K_{34}^2+K_{21}^4 & K_{33}^2+K_{22}^4 & 0 & K_{24}^4 & K_{23}^4 \\ 0 & 0 & 0 & K_{41}^3 & K_{42}^4 & 0 & K_{44}^4 & K_{43}^4 & 0 \\ 0 & 0 & 0 & K_{31}^3 & K_{32}^3+K_{41}^4 & K_{42}^4 & K_{34}^3 & K_{33}^3+K_{44}^4 & K_{43}^4 \\ 0 & 0 & 0 & 0 & K_{31}^4 & K_{32}^4 & 0 & K_{34}^4 & K_{33}^4 \end{bmatrix}\begin{Bmatrix} \psi_1 \\ \psi_2 \\ \psi_3 \\ \psi_4 \\ \psi_5 \\ \psi_6 \\ \psi_7 \\ \psi_8 \\ \psi_9 \end{Bmatrix} = \left(\frac{U_1\Omega_{ji}}{2}\right)\begin{Bmatrix} N_1^1 \\ N_2^1+N_1^2 \\ N_2^2 \\ N_4^1+N_1^3 \\ N_3^1+N_4^2+N_2^3+N_1^4 \\ N_3^2+N_2^4 \\ N_4^3 \\ N_3^3+N_4^4 \\ N_3^4 \end{Bmatrix} \tag{33}$$

Finally we evaluated the system matrix

$$\begin{bmatrix} 1.4167 & 1.375 & 0 & 0.75 & -0.70833 & 0 & 0 & 0 & 0 \\ 1.375 & 2.8334 & 1.125 & 0.625 & 1.3333 & 0.0833 & 0 & 0 & 0 \\ 0 & 1.125 & 1.9167 & 0 & 0.4583 & 00.0833 & 0 & 0 & 0 \\ 0.75 & 0.4583 & 0 & 2.8334 & 0.0833 & 0 & -3.25 & 3.2917 & 0 \\ -0.70833 & 1.3333 & 0.4583 & 0.0833 & 5.6668 & 3.0417 & 3.2917 & -6.6667 & 3.5417 \\ 0 & -0.4583 & 0.0833 & 0 & 0 & 3.8334 & 0 & 3.5417 & -3.9167 \\ 0 & 0 & 0 & -3.25 & 3.5417 & 0 & 9.4167 & -9.2917 & 0 \\ 0 & 0 & 0 & 3.2917 & -6.6667 & 3.5417 & -9.2917 & 10.8334 & -9.5417 \\ 0 & 0 & 0 & 0 & 3.5417 & -3.9167 & 0 & -9.5417 & 1.9167 \end{bmatrix} \begin{Bmatrix} \psi_1 \\ \psi_2 \\ \psi_3 \\ \psi_4 \\ \psi_5 \\ \psi_6 \\ \psi_7 \\ \psi_8 \\ \psi_9 \end{Bmatrix} = \begin{Bmatrix} 1588.6288 \\ 0 \\ 0 \\ 3177.2576 \\ 0 \\ 0 \\ 1588.6288 \\ 0 \\ 0 \end{Bmatrix} \quad (34)$$

$$\begin{Bmatrix} \psi_1 \\ \psi_2 \\ \psi_3 \\ \psi_4 \\ \psi_5 \\ \psi_6 \\ \psi_7 \\ \psi_8 \\ \psi_9 \end{Bmatrix} = \begin{bmatrix} 568.3382 \\ -898.4816 \\ 608.6242 \\ 2403.6911 \\ -305.0951 \\ -191.2748 \\ 1054.4221 \\ -59.4082 \\ -122.8500 \end{bmatrix} \quad (35)$$

RESULTS AND DISCUSSION

Applying the boundary conditions with respect to Figure 2 we obtained the following results as shown in Table 1:

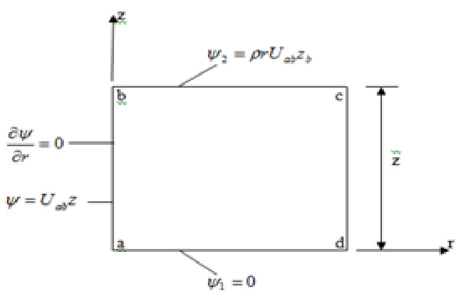

Fig 2: Computational domain and boundary conditions for the stream-function formulation.

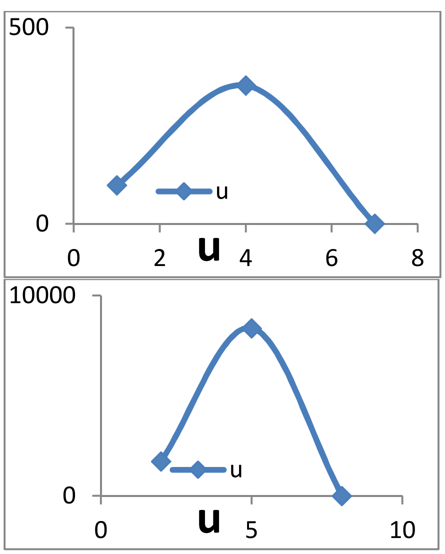

Fig 3: Graph of velocity against nodal values showing the Velocity profile at different cross section along the riser

The velocity profile at any cross section is parabolic in shape with the maximum velocity at the centre (Figure 3). The finite element solutions converged towards the exact solution (Figure 4).

Table 1: Finite Element solutions from the Analysis of Axisymmetric Flow of Air through the top riser of Casting using the Stream Function Model

Nodes	r (mm)	z (mm)	Stream function	Velocity (mm/s)
9	0	0	568.3382	0
8	0	1000	-898.4816	0
7	0	2000	608.6242	0
6	250	0	2403.6911	2775.9873
5	250	1000	-305.0951	8378.6391
4	250	2000	-191.2748	352.1123
3	500	0	1054.4221	963.4160
2	500	1000	-59.4082	1722.8620
1	500	2000	-122.8500	98.1312

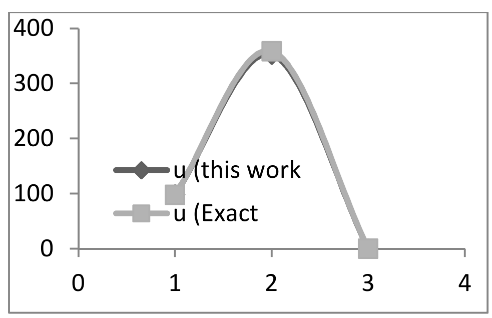

Fig 4: graph of velocity against nodal values showing the Velocity profile at different cross section of the riser this work and Exact solutions

The finite element results when compared with the experimental results (Inegbedion and Akpobi, 2017a) and the Mach number showed that the air flow in the casting mould was compressible.

Conclusion: In this work we have used the finite element method and the stream function model to establish the compressibility of air flow in casting mould. Results showed that the velocity profile at any cross section of the riser is parabolic in shape with the maximum velocity at the centre. Comparing results with exact solution shows that the finite element solution converged towards the exact solution. The finite element results were also compared with the experimental results obtained from the measurement of air velocity from the riser using a rotary vane anemometer.

REFERENCES

Aqida, SN; Ghazali, MI; Hashim, J (2004). Effects of porosity on mechanical properties of metal matrix composite: An overview. *J. Teknologi*, *40*(A): 17 – 32.

Feng, L (2008). Optimized Design of Gating/Riser System in Casting Based on CAD and Simulation Technology. MSc. Thesis, Worchester Polytechnic Institute.

Flinn, RA (1963). Fundamentals of Metal Casting, A'ddison-Wesley Publishing Co.

Inegbedion, F; Akpobi, JA (2017a). Determination of the Compressibility of Air in Casting Mould. Nigerian Research Journal of Engineering and Environmental Sciences, (*RJEES*) 2 (2): 524 – 529.

Inegbedion, F; Akpobi, JA (2017b). Stream Function Modelling of Compressible Axisymmetric Flow of Air through the Riser of Casting Mould. Transactions of the Nigerian Association of Mathematical Physics, (*Trans. of NAMP*) 5: 149 – 152.

Meir, GB (2013). Basics of Fluid Mechanics. *March, Orange Grove Books*, Chicago, Il.

Monroe, R (2005). *Porosity in Castings. AFS Transactions*. American foundry Society, Schaumburg, IL USA.

Peti, F and Grama, L (2011). Analyze of the Possible causes of Porosity Type Defects in Aluminium High Pressure Diecast Parts. Scientific Bulletin of the Petru Maior, University of Targu Mures

Reddy, JN (1993). An Introduction to the Finite Element Method, Second Edition, McGraw-Hill Inc.

Reddy, JN (2006). An Introduction to the Finite Element Method, Third Edition, International Edition McGraw-Hill Inc.

Scott, WD; Goodman, P (1979). Gas Generation at the Mold/Metal Interface. *1978 AFS Research Reports*, pp. 63-76.

Singiresu, SR (2004). The Finite Element Methods in Engineering, fourth edition, Elsevier Science and Technology Books Publisher.